Hindawi Publishing Corporation
International Journal of Photoenergy
Volume 2014, Article ID 270186, 6 pages
http://dx.doi.org/10.1155/2014/270186

Research Article

Love Wave Ultraviolet Photodetector Fabricated on a TiO_2/ST-Cut Quartz Structure

Walter Water,[1] Yi-Shun Lin,[2] and Chi-Wei Wen[1]

[1] *Department of Electronic Engineering, National Formosa University, Yunlin 632, Taiwan*
[2] *Institute of Electro-Optical and Materials Science, National Formosa University, Yunlin 632, Taiwan*

Correspondence should be addressed to Walter Water; wwater@nfu.edu.tw

Received 30 May 2014; Accepted 20 June 2014; Published 10 July 2014

Academic Editor: Teen-Hang Meen

A TiO_2 thin film deposited on a 90° rotated 42°45′ ST-cut quartz substrate was applied to fabricate a Love wave ultraviolet photodetector. TiO_2 thin films were grown by radio frequency magnetron sputtering. The crystalline structure and surface morphology of TiO_2 thin films were examined using X-ray diffraction, scanning electron microscope, and atomic force microscope. The effect of TiO_2 thin film thickness on the phase velocity, electromechanical coupling coefficient, temperature coefficient of frequency, and sensitivity of ultraviolet of devices was investigated. TiO_2 thin film increases the electromechanical coupling coefficient but decreases the temperature coefficient of frequency for Love wave propagation on the 90° rotated 42°45′ ST-cut quartz. For Love wave ultraviolet photodetector application, the maximum insertion loss shift and phase shift are 2.81 dB and 3.55 degree at the 1.35-μm-thick TiO_2 film.

1. Introduction

Titanium dioxide (TiO_2) is a wide gap semiconductor and has three kinds of crystallography structures named anatase, brookite, and rutile. Anatase phase has the most photocatalytic activity due to its larger band gap energy (3.2 eV) and rutile phase has higher refractive index and compact structure [1, 2]. TiO_2 was intensively investigated on various fields due to its strong mechanical and chemical stability, high dielectric constant, excellent photoelectric activity, and diverse nanostructures [3–5]. Ever since Fujishima et al. demonstrated photocatalytic activity of TiO_2[6], it became the most popular material for photocatalysis applications that can be applied to decomposite of a large variety of organic and inorganic compounds into environmentally friendly compounds. The optical absorption energies for photocatalytic activity of TiO_2 have been modified from the ultraviolet to the visible and near infrared by doping [7, 8]. The various surface morphologies and nanostructures of TiO_2 thin films were grown to increase the absorption ability for optical devices applications [9]. TiO_2 thin film can be synthesized using various approaches, such as chemical vapor deposition (CVD) [10], sol-gel process [11], pulsed laser deposition [12], hydrothermal method, and magnetron sputtering [13–15].

Surface acoustic wave (SAW) devices have been widely applied in wireless communication components, sensors, and actuators [16, 17]. Love wave is the one type of SAWs, which is a shear horizontal polarized wave, that has the highest sensitivity in a liquid environment among all known acoustic sensors due to the waveguiding effect [18, 19]. Love waves propagate in a layered structure consisting of a substrate and a layer on top of it. The layer acts as a guide, with the elastic waves generated in the substrate being coupled to the surface guiding layer [18].

Leaky waves of $LiTaO_3$ and $LiNbO_3$ and surface skimming bulk waves (SSBW) of ST-cut quartz have been used as substrates for Love wave devices applications [20–22]; typically ZnO, fused silica (SiO_2), and polymethylmethacrylate (PMMA) thin films have been used to construct the layered structure for the Love wave sensor [18, 23, 24]. SSBW transmitted on ST-cut quartz has higher wave velocity than other substrates. ZnO thin film is an excellent guiding layer for Love wave devices applications because it is a piezoelectric material and can be deposited as various surface

morphologies and nanostructures [25, 26]. But ZnO film presents a poor stability in the acid or alkaline solutions. TiO_2 thin films and TiO_2 nanowires have been applied for various types of UV photodetectors [10, 27], but the reports of Love wave type were few. The requirements of guiding layer for a Love wave device application are being rigid, dense, and stable and having low radiation loss. Although TiO_2 is not a piezoelectric material, its strong mechanical and chemical stability, excellent photoelectric activity, and ease of synthesizing the various surface morphologies with nanostructures provide the potential as the guiding and sensing layer for Love wave sensors applications.

2. Experimental

The Love wave devices were fabricated on ST-cut (42°45′) quartz substrates (12 mm × 13 mm × 0.5 mm) with a propagation direction perpendicular to the crystallographic x-axis (90° rotated). The input and output interdigital transducers (IDTs) consisted of 30 finger pairs with an electrode width of 10 μm and separation of 10 μm, yielding a periodicity of 40 μm. The IDT aperture was 4 mm and the center to center of separation was 6.2 mm. The IDTs were made of 200 nm sputtered titanium. After the contact electrode of IDTs with a protection, the TiO_2 films were deposited by RF magnetron sputtering using a TiO_2 target (99.9%). In the film deposition process, sputtering power was 350 W, sputtering pressure was 1.33 Pa, O_2/Ar ratio was 0.25, distance between substrate and target was 70 mm, and the substrate was not heated. The deposition rates were controlled at approximately 170 nm/hour. Figure 1 presents the structure and pattern of the Love wave device.

The crystalline structure and orientation of the TiO_2 films were examined by X-ray diffraction (XRD) (Shimadzu XRD-6000). The surface morphology of the TiO_2 films was analyzed using field-emission scanning electron microscopy (FESEM) (Hitachi S4800-I) and atomic force microscopy techniques (DI D3100). Frequency response, phase of transmitted signals, wave velocities, electromechanical coupling coefficients, UV responses, and temperature coefficients of frequency of Love wave devices were measured by the network analyzer (Agilent E5062A). The error bars were calculated as two devices with the same parameters for measuring three times, respectively.

3. Results and Discussion

3.1. Crystalline Structure and Surface Morphology. Figure 2 presents the XRD patterns of TiO_2 thin films with different thicknesses deposited on quartz substrates. The TiO_2 thin film at 1.35-μm thickness shows an anatase structure and the major reflection planes are (101), (004), (112), (200), and (211), respectively. The films at 0.50- and 1.60-μm thicknesses present an amorphous structure. Figure 3 shows the SEM images of TiO_2 films with various thicknesses. The surface morphology is transferred greatly due to the films' thickness. The 0.50-μm thick TiO_2 thin film has a smooth surface and a small columnar size. When thickness reaches 0.85 and 1.35 μm, the polyhedrons with a sharp shape are grown on the surface and the columnar size increases obviously. The surface roughness of films turns into rough with increasing thickness. The root mean square values of surface roughness are presented in Table 1.

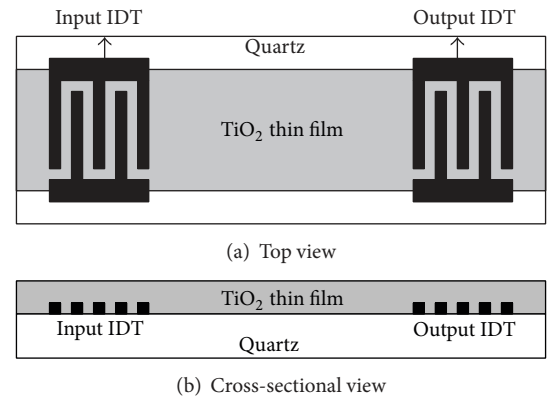

Figure 1: Structure of the Love wave device.

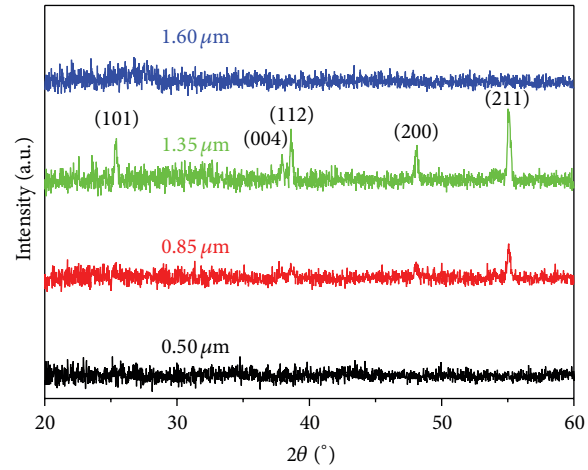

Figure 2: XRD patterns of TiO_2 thin films with various thicknesses.

Table 1: The root mean square values and phase velocities of TiO_2 thin films deposited on quartz substrate with various thicknesses.

Thickness (μm)	Root mean square value (nm)	Phase velocity (m/s)
0.50	0.47	4907
0.85	2.84	4814
1.35	3.34	4787
1.60	5.87	4725
2.50	10.81	4356

3.2. Love Wave Device with TiO_2 Guiding Layer. Figure 4 shows the frequency response and phase of transmitted signal (S_{21}) for device with a 1.6-μm thick TiO_2 film. The phase velocity of a blank ST-cut (42°45′) quartz for X-propagation is 5060 m/s; the phase velocity decreases with increasing thickness of TiO_2 thin film and approaches 4356 m/s for

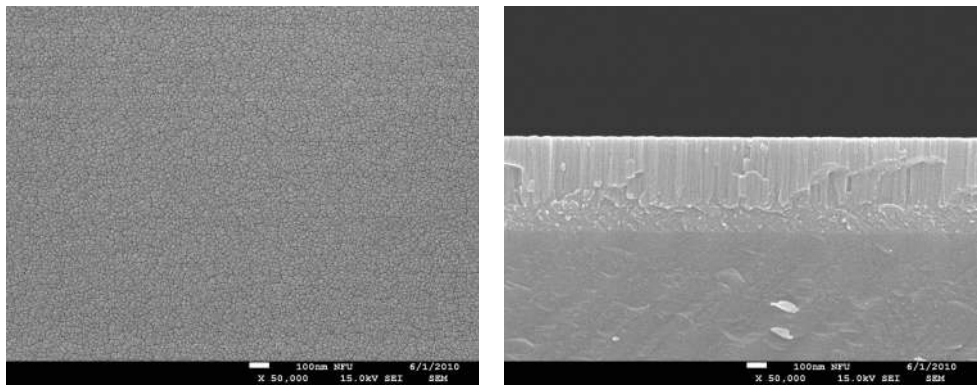

(a) Thickness of 0.50 μm

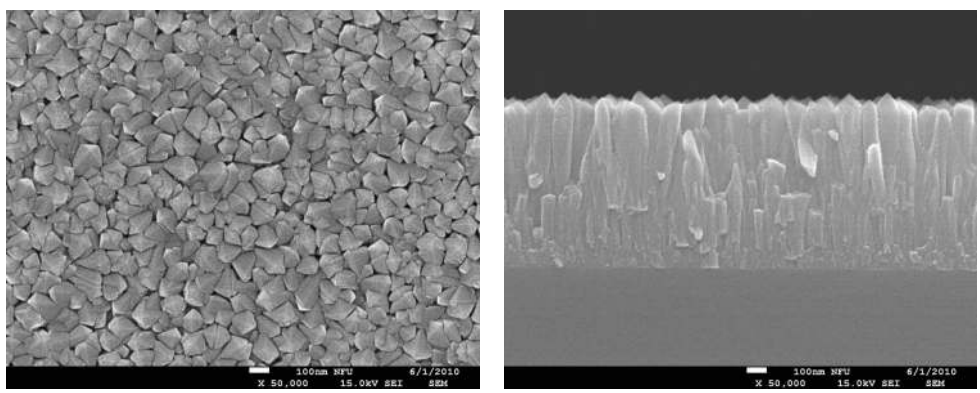

(b) Thickness of 0.85 μm

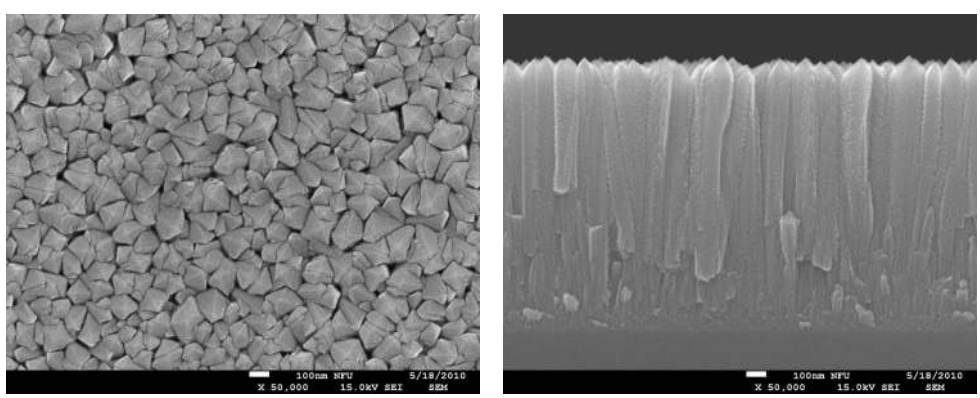

(c) Thickness of 1.35 μm

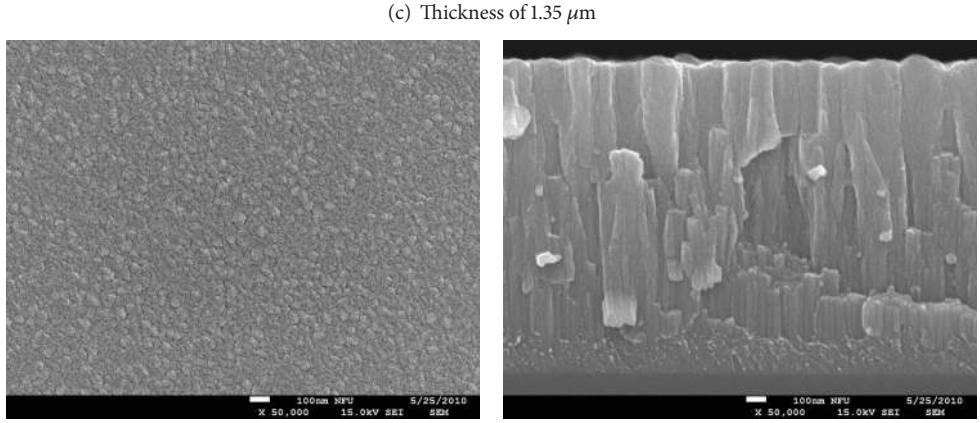

(d) Thickness of 1.60 μm

Figure 3: SEM images of TiO_2 thin films with various thicknesses.

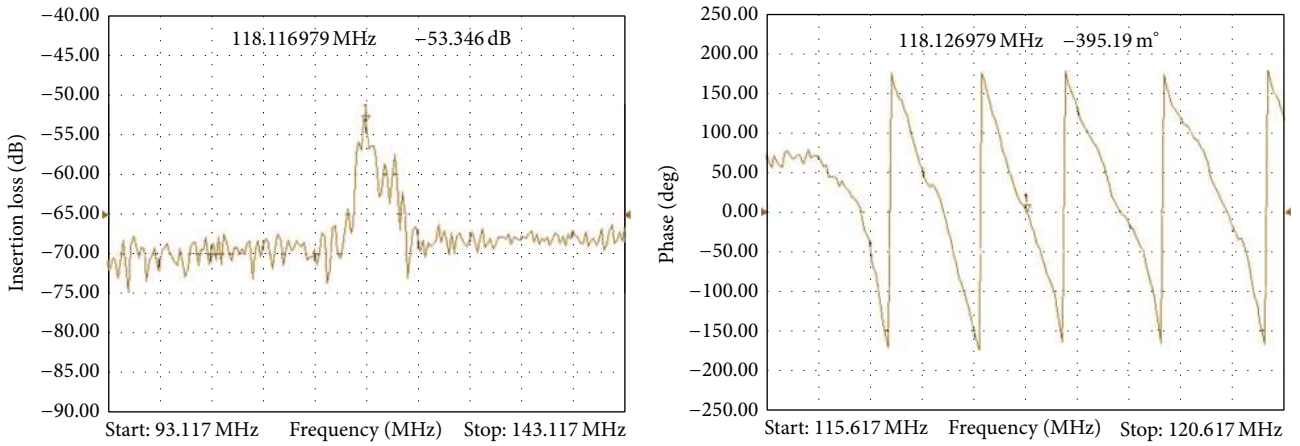

(a) Frequency response of transmitted signal

(b) Phase of transmitted signal

Figure 4: Frequency response and phase of transmitted signal (S_{21}) of 1.6-μm thick TiO_2 film.

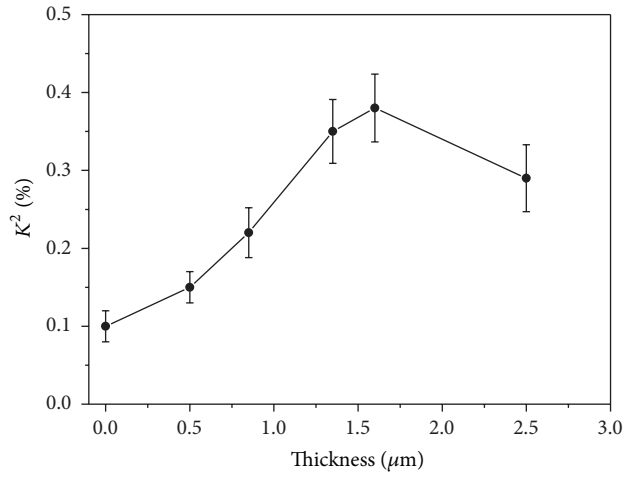

Figure 5: Electromechanical coupling coefficients of devices with different thicknesses of TiO_2 thin films.

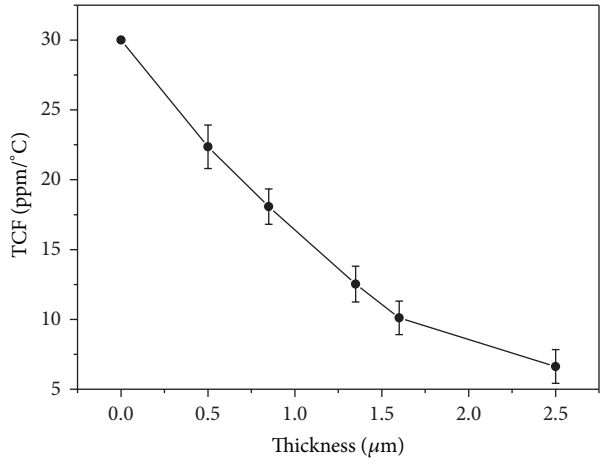

Figure 6: Temperature coefficients of frequency of devices with different thicknesses of TiO_2 thin films.

the 2.5-μm thick TiO_2 film deposited. The phase velocities versus films thicknesses are shown in Table 1.

The electromechanical coupling coefficient (k^2) was obtained as follows:

$$k^2 = \frac{\pi}{4N}\frac{\mathrm{Ga}}{B}, \tag{1}$$

where N is the number of IDT finger pairs and Ga and B are radiation resistance and susceptance, respectively [28]. Figure 5 shows the electromechanical coupling coefficients of devices with different thicknesses of TiO_2 thin films. Although TiO_2 thin film is not a piezoelectric material, the electromechanical coupling coefficients of devices increase with increasing thicknesses due to the waveguide effect and the maximum value is 0.38% at the 1.6-μm thick TiO_2 film.

The temperature coefficients of frequency (TCF) were calculated by substituting the center frequencies at 30, 50, and 70°C into the following equation:

$$\mathrm{TCF} = \frac{F\left(70^\circ\mathrm{C}\right) - F\left(30^\circ\mathrm{C}\right)}{40 \times F\left(50^\circ\mathrm{C}\right)}. \tag{2}$$

Figure 6 shows the TCFs of devices with different thicknesses of TiO_2 thin films. The 90° rotated 42°45′ ST-cut quartz reported in the literature showed a relatively high TCF about +30 ppm/°C [16]. This TCF value decreases by means of a TiO_2 layer with a low TCF value and reduces to +6.6 ppm/°C at 2.5-μm thick TiO_2 film.

3.3. Characteristics of the Love Wave Ultraviolet Photodetector. The band gap of TiO_2 thin film with anatase phase is about 3.2 eV; carriers' concentrations are increased when the TiO_2 thin film is exposed to UV illumination. When Love wave

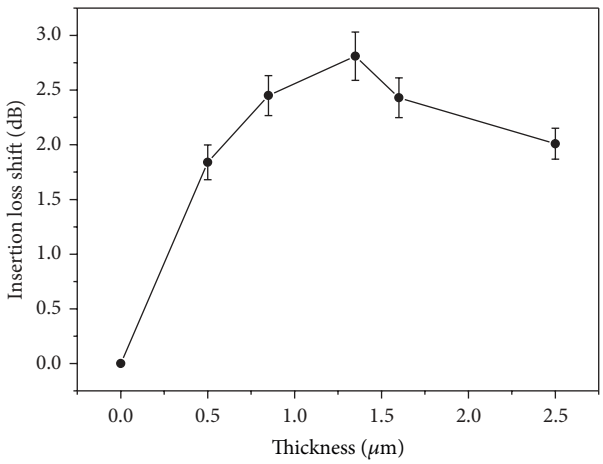

Figure 7: Insertion loss shifts of devices with different thicknesses of TiO_2 thin films after 365 nm UV illumination for 30 seconds.

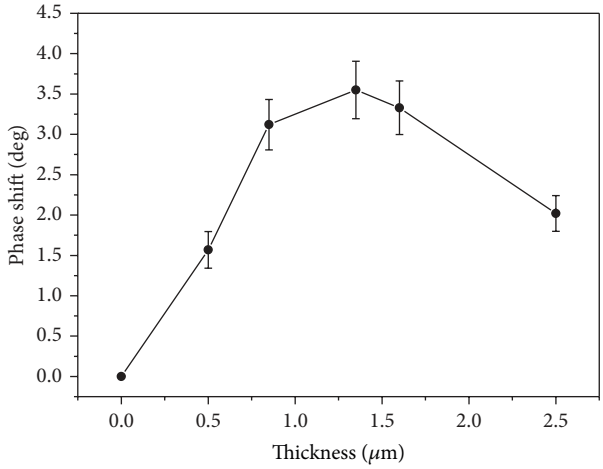

Figure 8: Phase shifts of devices with different thicknesses of TiO_2 thin films after 365 nm UV illumination for 30 seconds.

is transmitted in a guiding layer, the variations in electrical properties of the guiding layer affect the characteristics of wave propagation sensitively. The wave velocity will decrease when the guiding layer becomes a higher conducting film due to the capacitance increasing and insertion loss of transmission signal will shift due to the variation of impedance [16]. Figure 7 shows the insertion loss shifts with different thicknesses of TiO_2 thin films after 365 nm UV illumination for 30 seconds. The maximum change is 2.81 dB at the 1.35-μm thick TiO_2 film. The main vibration and transmission of Love wave is in the interface between the guiding layer and substrate. The over thick guiding layer may be reducing and slowing the variations of conductivity in the interface. Figure 8 shows the phase shifts with different thickness of TiO_2 thin film after 365 nm UV illumination for 30 seconds. The maximum phase shift is 3.55 degree at the 1.35-μm thick TiO_2 film. Compare ZnO thin film of our previous results as the same structure and IDT pattern, the maximum phase shift of 1.0-μm thick ZnO film after 30 seconds under 365 nm UV illumination was below 1 degree [23]. The TiO_2 thin film provides the good potential for Love wave UV photodetector application.

4. Conclusions

The Love wave ultraviolet photodetector that used TiO_2 thin film and 90° rotated 42°45′ ST-cut quartz substrate was proposed. The effect of thickness of TiO_2 thin film on the phase velocity, electromechanical coupling coefficient, temperature coefficient of frequency, and ultraviolet sensitivity of device was investigated. Although TiO_2 thin film is not a piezoelectric material, the electromechanical coupling coefficient increases from 0.10% of blank quartz substrate to 0.38% at the 1.6-μm thick TiO_2 film deposited due to the waveguiding effect. The temperature coefficient of frequency decreases with increasing thickness of TiO_2 thin film. The ultraviolet sensitivity is affected sensitively by the thickness of the TiO_2 thin film; the maximum insertion loss shift and phase shift are 2.81 dB and 3.55 degree at the 1.35-μm thick TiO_2 film.

Conflict of Interests

The authors declare that there is no conflict of interests regarding the publication of this paper.

Acknowledgment

The authors would like to thank the National Science Council of China, Taiwan, for financially supporting this research under Grant no. NSC-101-2221-E-150-044.

References

[1] M. H. Habibi, N. Talebian, and J. Choi, "The effect of annealing on photocatalytic properties of nanostructured titanium dioxide thin films," *Dyes and Pigments*, vol. 73, no. 1, pp. 103–110, 2007.

[2] C. Sarra-Bournet, C. Charles, and R. Boswell, "Low temperature growth of nanocrystalline TiO_2 films with Ar/O_2 low-field helicon plasma," *Surface and Coatings Technology*, vol. 205, no. 15, pp. 3939–3946, 2011.

[3] H. Rath, P. Dash, T. Som et al., "Structural evolution of TiO_2 nanocrystalline thin films by thermal annealing and swift heavy ion irradiation," *Journal of Applied Physics*, vol. 105, no. 7, Article ID 074311, 2009.

[4] A. K. Pradhan, D. Hunter, J. B. Dadson et al., "Structural evolution of TiO_2 nanocrystalline thin films by thermal annealing and swift heavy ion irradiation," *Applied Physics Letters*, vol. 86, Article ID 222503, 2005.

[5] J. E. Lyon, M. K. Rayan, M. M. Beerbom, and R. Schlaf, "Electronic structure of the indium tin oxide/nanocrystalline anatase (TiO_2)/ruthenium-dye interfaces in dye-sensitized solar cells," *Journal of Applied Physics*, vol. 104, no. 7, Article ID 073714, 2008.

[6] A. Fujishima, K. Hashimoto, and T. Watanabe, *TiO_2 Photocatalysis: Fundamentals and Applications*, BKC, Tokyo, Japan, 1999.

[7] D. Wojcieszak, M. Mazur, M. Kurnatowska et al., "Influence of Nd-doping on photocatalytic properties of TiO_2 nanoparticles

and thin film coatings," *International Journal of Photoenergy*, vol. 2014, Article ID 463034, 10 pages, 2014.

[8] Y. Nakano, T. Morikawa, T. Ohwaki, and Y. Taga, "Deep-level optical spectroscopy investigation of N-doped TiO_2 films," *Applied Physics Letters*, vol. 86, no. 13, Article ID 132104, 2005.

[9] H. C. Chang, M. J. Twu, C. Y. Hsu, R. Q. Hsu, and C. G. Kuo, "Improved performance for dye-sensitized solar cells using a compact TiO_2 layer grown by sputtering," *International Journal of Photoenergy*, vol. 2014, Article ID 380120, 8 pages, 2014.

[10] X. Kong, C. Liu, W. Dong et al., "Metal-semiconductor-metal TiO_2 ultraviolet detectors with Ni electrodes," *Applied Physics Letters*, vol. 94, no. 12, Article ID 123502, 2009.

[11] W. Zhang, Q. Li, and W. Liu, "Some influencing factors on photocatalytic activity of TiO_2 film prepared using sol-gel method," *Advanced Materials Research*, vol. 433–440, pp. 362–366, 2012.

[12] E. György, G. Socol, E. Axente, I. N. Mihailescu, C. Ducu, and S. Ciuca, "Anatase phase TiO_2 thin films obtained by pulsed laser deposition for gas sensing applications," *Applied Surface Science*, vol. 247, no. 1–4, pp. 429–433, 2005.

[13] S. Biswas, K. Prabakar, T. Takahashi, T. Nakashima, Y. Kubota, and A. Fujishima, "Study of photocatalytic activity of TiO_2 thin films prepared in various Ar O_2 ratio and sputtering gas pressure," *Journal of Vacuum Science and Technology A*, vol. 25, no. 4, pp. 912–916, 2007.

[14] Q. Ye, P. Y. Liu, Z. F. Tang, and L. Zhai, "Hydrophilic properties of nano-TiO_2 thin films deposited by RF magnetron sputtering," *Vacuum*, vol. 81, no. 5, pp. 627–631, 2007.

[15] O. van Overschelde, G. Guisbiers, F. Hamadi, A. Hemberg, R. Snyders, and M. Wautelet, "Alternative to classic annealing treatments for fractally patterned TiO_2 thin films," *Journal of Applied Physics*, vol. 104, no. 10, Article ID 103106, 2008.

[16] C. K. Campbell, *Surface Acoustic Wave Devices for Mobile and Wireless Communications*, Academic Press, New York, NY, USA, 1998.

[17] D. S. Ballantine, R. M. White, S. J. Martin et al., *Acoustic Wave Sensors-Theory, Design and Physico-Chemical Applications*, Academic Press, New York, NY, USA, 1997.

[18] J. Du, G. L. Harding, J. A. Ogilvy, P. R. Dencher, and M. Lake, "A study of Love-wave acoustic sensors," *Sensors and Actuators A*, vol. 56, no. 3, pp. 211–219, 1996.

[19] Z. Zhang, Z. Wen, and C. Wang, "Investigation of surface acoustic waves propagating in ZnO-SiO_2-Si multilayer structure," *Ultrasonics*, vol. 53, no. 2, pp. 363–368, 2013.

[20] Y. Wang, S. Y. Zhang, F. M. Zhou, L. Fan, Y. Yang, and C. Wang, "Love wave hydrogen sensors based on ZnO nanorod film/36YX-$LiTaO_3$ substrate structures operated at room temperature," *Sensors and Actuators, B: Chemical*, vol. 158, no. 1, pp. 97–103, 2011.

[21] N. Barié, U. Stahl, and M. Rapp, "Vacuum-deposited wave-guiding layers on STW resonators based on $LiTaO_3$ substrate as love wave sensors for chemical and biochemical sensing in liquids," *Ultrasonics*, vol. 50, no. 6, pp. 606–612, 2010.

[22] K. Kalantar-Zadeh, W. Woldarski, Y. Y. Chen, B. N. Fry, and K. Galatsis, "Novel Love mode surface acoustic wave based immunosensors," *Sensors and Actuators B: Chemical*, vol. 91, no. 1–3, pp. 143–147, 2003.

[23] W. Water and R.-Y. Jhao, "Application of ZnO nanorods synthesized on 64◦ Y-cut $LiNbO_3$ to surface acoustic wave ultraviolet photodetector," *Sensors and Actuators B: Chemical*, vol. 173, pp. 310–315, 2012.

[24] G. L. Harding and J. Du, "Design and properties of quartz-based Love wave acoustic sensors incorporating silicon dioxide and PMMA guiding layers," *Smart Materials and Structures*, vol. 6, no. 6, pp. 716–720, 1997.

[25] H. Pang, Y. Fu, Z. Li et al., "Love mode surface acoustic wave ultraviolet sensor using ZnO films deposited on 36° Y-cut $LiTaO_3$," *Sensors and Actuators, A: Physical*, vol. 193, pp. 87–94, 2013.

[26] A. Talbi, F. Sarry, M. Elhakiki et al., "ZnO/quartz structure potentiality for surface acoustic wave pressure sensor," *Sensors and Actuators A: Physical*, vol. 128, no. 1, pp. 78–83, 2006.

[27] T. Tsai, S. Chang, W. Weng et al., "A visible-blind TiO_2 nanowire photodetector," *Journal of the Electrochemical Society*, vol. 159, no. 4, pp. J132–J135, 2012.

[28] W. R. Smith, H. M. Gerard, J. H. Collins, T. M. Reeder, and H. J. Shaw, "Analysis of interdigital surface wave transducers by use of an equivalent circuit model," *IEEE Transactions on Microwave and Theory Techniques*, vol. 17, no. 11, pp. 856–864, 1969.